Electronic Transactions on Numerical Analysis.
Volume 32, pp. 106-122, 2008.
Copyright © 2008, Kent State University.
ISSN 1068-9613.

ETNA
Kent State University
etna@mcs.kent.edu

LOCAL PROJECTION STABILIZATION FOR INCOMPRESSIBLE FLOWS: EQUAL-ORDER VS. INF-SUP STABLE INTERPOLATION*

G. LUBE†, G. RAPIN†, AND J. LÖWE†

Abstract. A standard approach to the non-stationary, incompressible Navier-Stokes model is to split the problem into linearized auxiliary problems of Oseen type. In this paper, a unified numerical analysis for finite element discretizations using the local projection stabilization method with either equal-order or inf-sup stable velocity-pressure pairs in the case of continuous pressure approximation is presented. Moreover, a careful comparison of both variants is given.

Key words. incompressible flows, Oseen model, stabilized FEM, local projection stabilization

AMS subject classifications. 65M60, 65N15, 76M10

1. Introduction. Consider the non-stationary incompressible Navier-Stokes model

$$\begin{aligned} \partial_t \boldsymbol{u} - \nu \triangle \boldsymbol{u} + (\boldsymbol{u}\cdot\nabla)\boldsymbol{u} + \nabla p &= \tilde{\boldsymbol{f}} && \text{in } \Omega \times (0,T), \\ \nabla \cdot \boldsymbol{u} &= 0 && \text{in } \Omega \times (0,T), \end{aligned}$$

for velocity $\boldsymbol{u}$ and pressure p in a bounded domain $\Omega \subset \mathbb{R}^d$, $d = 2, 3$. A usual approach is to semi-discretize in time first with an A-stable implicit scheme [17]. In each time step, the resulting problems can be solved via a fixed-point or Newton-type scheme [17, 22]. This leads to auxiliary problems of Oseen type

$$L_{Os}(\boldsymbol{u}, p) := -\nu \triangle \boldsymbol{u} + (\boldsymbol{b}\cdot\nabla)\boldsymbol{u} + \sigma \boldsymbol{u} + \nabla p = \boldsymbol{f} \qquad \text{in } \Omega, \tag{1.1}$$

$$\nabla \cdot \boldsymbol{u} = 0 \qquad \text{in } \Omega, \tag{1.2}$$

with a new right-hand side $\boldsymbol{f} \in [L^2(\Omega)]^d$, with coefficients $\boldsymbol{b} \in [H^1(\Omega) \cap L^\infty(\Omega)]^d$, and $\sigma \geq 0$ (stemming from time discretization).

The Galerkin approximation of (1.1), (1.2) may suffer from two problems: violation of the discrete inf-sup (or Babuška-Brezzi) stability condition and dominating advection, i.e., $\nu \ll \|\boldsymbol{b}\|_{[L^\infty(\Omega)]^d}$. The traditional way to cope with both problems in a common framework is the combination of the streamline-upwind/Petrov-Galerkin method (SUPG) [7] and the pressure-stabilization/Petrov-Galerkin method (PSPG) [18]. An overview about residual stabilized methods can be found in [5, 24]. More recent results for h-p finite elements are proven in [20].

This class of residual based stabilization techniques is still quite popular, since they are robust and easy to implement. Nevertheless, they have severe drawbacks which mainly stem from the strong coupling between velocity and pressure in the stabilization terms [5]. Therefore, other stabilization techniques have appeared recently, in particular the edge-stabilization method [5, 8] and variational multiscale (VMS) methods [9, 13, 15, 16]. We emphasize that almost all stabilization methods can be interpreted as special VMS methods. The key idea of VMS methods is a separation of scales: large scales, small scales, and unresolved scales. The influence of the unresolved scales on the other scales has to be modeled. Mostly, it is assumed that the unresolved scales do not influence the large scales.

*Received November 29, 2007. Accepted for publication July 4, 2008. Published online on February 9, 2009. Recommended by A. Rösch.

†Department of Mathematics, NAM, University of Göttingen, Lotzestrasse 16-18, D-37083 Göttingen, Germany (lube, grapin, loewe@math.uni-goettingen.de).

Currently, there are two variants to apply VMS methods to the full Navier-Stokes model. In most papers, an equal-order interpolation of velocity-pressure is applied; see, e.g., [2, 9]. Besides the rather simple implementation into existing codes, a formal reason is appearantly that in the Euler limit $\nu \to 0$ no second-order derivatives occur. Other authors prefer discrete inf-sup stable velocity-pressure pairs [16] as this is the "natural" choice from regularity point of view for fixed $\nu > 0$. A comparison of both approaches is still missing.

Local projection stabilization (LPS) as special VMS-type methods are of current interest [4, 21]. Here the influence of the unresolved scales on the small scales is modeled by additional artificial diffusion terms for the small scales. In particular, the sub-grid viscosity model [14] can be interpreted as a special LPS method. In Section 3 of this paper, we present a unified theory of LPS methods for equal-order and inf-sup stable pairs in the case of continuous pressure approximation. In Section 4, a comparison of both variants is given with respect to theory and simple numerical experiments.

Throughout this paper, the standard notation $\|\cdot\|_{k,G}$ for the norm in the Sobolev spaces $H^k(G) = W^{k,2}(G), G \subseteq \Omega$ are used. The L^2-inner product in a domain G is denoted by $(\cdot,\cdot)_G$. The norm in $L^\infty(G)$ is denoted by $\|\cdot\|_{L^\infty(G)}$. For $G = \Omega$, the index is eventually omitted.

2. Variational formulation and stabilization. Here, the basic Galerkin finite element formulation and its stabilized variants via local projection (LPS) are introduced. Moreover, different technical tools are given.

2.1. Basic Galerkin approximation. The basic variational formulation for the Oseen problem (1.1), (1.2) with homogeneous Dirichlet data reads: Find $U = (\boldsymbol{u}, p) \in \boldsymbol{V} \times Q := [H_0^1(\Omega)]^d \times L_0^2(\Omega)$, such that

$$\underbrace{(\nu\nabla\boldsymbol{u}, \nabla\boldsymbol{v})_\Omega + ((\boldsymbol{b}\cdot\nabla)\boldsymbol{u} + \sigma\boldsymbol{u}, \boldsymbol{v})_\Omega - (p, \nabla\cdot\boldsymbol{v})_\Omega + (q, \nabla\cdot\boldsymbol{u})_\Omega}_{=:A(U,V)} = \underbrace{(\boldsymbol{f}, \boldsymbol{v})_\Omega}_{=:L(V)} \tag{2.1}$$

for all $V = (\boldsymbol{v}, q) \in \boldsymbol{V} \times Q$.

ASSUMPTION 2.1. Let $\Omega \subset \mathbb{R}^d, d \in \{2,3\}$, be a bounded, polyhedral domain. Moreover, assume that $\nu \in L^\infty(\Omega)$ with $\nu > 0$ in Ω, $\boldsymbol{f} \in [L^2(\Omega)]^d$, $\boldsymbol{b} \in [L^\infty(\Omega) \cap H^1(\Omega)]^d$ with $\nabla\cdot\boldsymbol{b} = 0$ a.e. in Ω and constant $\sigma \geq 0$.

REMARK 2.2. Usually, $\boldsymbol{b}$ is a finite element solution of the Oseen equation. In particular, there holds $(\nabla\cdot\boldsymbol{b}, q_h) = 0$ for certain test functions q_h. Therefore $\nabla\cdot\boldsymbol{b}$ is small but does not vanish in general. A remedy for iterative methods within a Navier-Stokes simulation is to replace $((\mathbf{b}\cdot\nabla)\mathbf{u}, \mathbf{v})_\Omega$ by $\frac{1}{2}((\mathbf{b}\cdot\nabla)\mathbf{u}, \mathbf{v})_\Omega - \frac{1}{2}((\mathbf{b}\cdot\nabla)\mathbf{v}, \mathbf{u})_\Omega - \frac{1}{2}((\nabla\cdot\mathbf{b})\mathbf{u}, \mathbf{v})_\Omega$.

REMARK 2.3. It is possible to extend the analysis in this paper to a situation resulting from Newton iteration including the term $(\boldsymbol{u}\cdot\nabla)\boldsymbol{b}$. A small time step, resulting in a sufficiently large $\sigma \geq 2\|\nabla\boldsymbol{b}\|_{(L^\infty(\Omega))^{d\times d}}$, ensures coercivity of the Oseen operator since $(\sigma\boldsymbol{u}, \boldsymbol{u})_\Omega + ((\boldsymbol{u}\cdot\nabla)\boldsymbol{b}, \boldsymbol{u})_\Omega \geq (\sigma - \|\nabla\boldsymbol{b}\|_{(L^\infty(\Omega))^{d\times d}})\|\boldsymbol{u}\|_0^2 \geq \frac{1}{2}\sigma\|\boldsymbol{u}\|_0^2$.

We consider a shape-regular, admissible decomposition $\mathcal{T}_h$ of Ω into d-dimensional simplices, quadrilaterals in the two-dimensional case or hexahedra for three dimensions. Let h_T be the diameter of a cell $T \in \mathcal{T}_h$ and h be the maximum of all h_T, $T \in \mathcal{T}_h$. Let $\hat{T}$ be a reference element of the decomposition $\mathcal{T}_h$.

We set

$$P_{k,\mathcal{T}_h} := \{v_h \in L^2(\Omega) \mid v_h|_T \circ F_T \in \mathbb{P}_k(\hat{T})\ , T \in \mathcal{T}_h\},$$

where $\mathbb{P}_k(\hat{T})$ is the space of all polynomials of degree k defined on $\hat{T}$, and

$$\tilde{Q}_{k,\mathcal{T}_h} := \{v_h \in L^2(\Omega) \mid v_h|_T \circ F_T \in \mathbb{Q}_k(\hat{T})\ , T \in \mathcal{T}_h\},$$

with $\mathbb{Q}_k(\hat{T})$ the space of all polynomials on $\hat{T}$ with maximal degree k in each coordinate direction. The finite element space of the velocity is given by $\mathbf{V}_{h,k_u} = [\tilde{Q}_{k_u,\mathcal{T}_h}]^d \cap \boldsymbol{V}$ or $\mathbf{V}_{h,k_u} = [P_{k_u,\mathcal{T}_h}]^d \cap \boldsymbol{V}$ with scalar components Y_{h,k_u} of $\mathbf{V}_{h,k_u}$.

For simplicity, we restrict the analysis to continuous discrete pressure spaces $Q_{h,k_p} = \tilde{Q}_{k_p,\mathcal{T}_h} \cap C(\overline{\Omega})$ or $Q_{h,k_p} = P_{k_p,\mathcal{T}_h} \cap C(\overline{\Omega})$. For an extension to discontinuous pressure spaces, we refer to [23].

The subsequent numerical analysis takes advantage of the inverse inequality

$$\exists \mu_{inv} \mid \quad |\boldsymbol{v}|_{1,T} \leq \mu_{inv} k_u^2 h_T^{-1} \|\boldsymbol{v}\|_{0,T}, \quad \forall T \in \mathcal{T}_h, \ \forall \boldsymbol{v}_h \in \boldsymbol{V}_{h,k_u}, \tag{2.2}$$

and of the interpolation properties of the finite element space $\mathbf{V}_{h,k_u}$. For the Scott-Zhang quasi-interpolant operator I^u_{h,k_u} [26, 1], one obtains for $v \in H^1_0(\Omega) \cap H^t(\Omega)$, $t > \frac{1}{2}$ with $v|_{\omega_T} \in H^r(\omega_T)$, $r \geq t$, on the patches $\omega_T := \bigcup_{\overline{T'} \cap \overline{T} \neq \emptyset} T'$,

$$\exists C > 0 \mid \quad \|v - I^u_{h,k_u} v\|_{m,T} \leq C \frac{h_T^{l-m}}{k_u^{r-m}} \|v\|_{r,\omega_T}, \quad 0 \leq m \leq l = \min(k_u + 1, r). \tag{2.3}$$

This property can be extended to the vector-valued case with $\boldsymbol{I}^u_{h,k_u} : \boldsymbol{V} \to \boldsymbol{V}_h$. Similarly, an interpolation operator I^p_{h,k_p} satisfying (2.3) can be defined for the pressure.

2.2. Local projection stabilization (LPS). The idea of LPS-methods is to split the discrete function spaces into small and large scales and to add stabilization terms of diffusion-type acting only on the small scales. Consider two obvious choices of the large scale space:

(i) The first variant [4, 6, 21] is to determine the large scales with the help of a coarse mesh. The coarse mesh $\mathcal{M}_h = \{M_i\}_{i \in I}$ is constructed by coarsening the basic mesh $\mathcal{T}_h$, such that each macro element $M \in \mathcal{M}_h$ with diameter h_M is the union of one or more neighboring cells $T \in \mathcal{T}_h$. Assume that the decomposition $\mathcal{M}_h$ of Ω is non-overlapping and shape-regular. Moreover, the interior cells are supposed to be of the same size as the macro cell:

$$\exists C > 0 \mid \quad h_M \leq C h_T, \quad \forall T \in \mathcal{T}_h, M \in \mathcal{M}_h, \text{ with } T \subset M. \tag{2.4}$$

Following the approach in [21] we define the discrete space D^u_h for the velocity as a discontinuous finite element space defined on the macro partition $\mathcal{M}_h$. The restriction on a macro-element $M \in \mathcal{M}_h$ is denoted by $D^u_h(M) := \{v_h|_M \mid v_h \in D^u_h\}$.

The next ingredient is a local projection $\pi^u_M : L^2(M) \to D^u_h(M)$, which defines the global projection $\pi^u_h : L^2(\Omega) \to D^u_h$ by $(\pi^u_h v)|_M := \pi^u_M(v|_M)$ for all $M \in \mathcal{M}_h$. Denoting the identity on $L^2(\Omega)$ by id, the associated fluctuation operator $\kappa^u_h : L^2(\Omega) \to L^2(\Omega)$ is defined by $\kappa^u_h := id - \pi^u_h$. These operators are applied to vector-valued functions in a component-wise manner. This is indicated by boldface notation, e.g., $\boldsymbol{\pi}^u_h : [L^2(\Omega)]^d \to [D^u_h]^d$ and $\boldsymbol{\kappa}^u_h : [L^2(\Omega)]^d \to [L^2(\Omega)]^d$.

(ii) The second choice [10, 21] consists of choosing a finite element discretization D^u_h of lower order on the original mesh $\mathcal{T}_h$ or by enriching the spaces $\boldsymbol{V}_{h,k_u}$ and Q_{h,k_p}. The same abstract framework as in the first approach can be used by setting $\mathcal{M}_h = \mathcal{T}_h$.

Analogously a discrete space D^p_h and a fluctuation operator κ^p_h can be defined. The stabilized discrete formulation reads: find $U_h = (\boldsymbol{u}_h, p_h) \in \boldsymbol{V}_{h,k_u} \times Q_{h,k_p}$, such that

$$A(U_h, V_h) + S_h(U_h, V_h) = L(V_h), \qquad \forall V_h = (v_h, q_h) \in \boldsymbol{V}_{h,k_u} \times Q_{h,k_p}, \tag{2.5}$$

where the additional stabilization term is given by

$$\begin{aligned} S_h(U_h, V_h) := \sum_{M \in \mathcal{M}_h} \Big[& \tau_M (\boldsymbol{\kappa}^u_h ((\boldsymbol{b} \cdot \nabla)\boldsymbol{u}_h), \boldsymbol{\kappa}^u_h ((\boldsymbol{b} \cdot \nabla)\boldsymbol{v}_h))_M \\ & + \mu_M (\kappa^p_h (\nabla \cdot \boldsymbol{u}_h), \kappa^p_h (\nabla \cdot \boldsymbol{v}_h))_M + \alpha_M (\boldsymbol{\kappa}^u_h(\nabla p_h), \boldsymbol{\kappa}^u_h(\nabla q_h))_M \Big]. \end{aligned} \tag{2.6}$$

ETNA
Kent State University
etna@mcs.kent.edu

REMARK 2.4. Another variant is to replace the first right-hand side term of $S_h(\cdot,\cdot)$ by

$$\sum_{M\in\mathcal{M}_h} \delta_M(\boldsymbol{\kappa}_h^u(\nabla \boldsymbol{u}_h), \boldsymbol{\kappa}_h^u(\nabla \boldsymbol{v}_h))_M;$$

see the corresponding result in Remark 3.9.

The constants τ_M, μ_M, α_M, and δ_M will be determined later, based on an a priori estimate. Notice that the stabilization $S_h(\cdot,\cdot)$ acts solely on the small scales. Of course, there are some more degrees of freedom in the choice of S_h; see also [4, 21].

In order to control the consistency error of the κ_h^u-dependent stabilization terms, the space D_h^u has to be large enough; more precisely we assume the following.

ASSUMPTION 2.5. The fluctuation operator κ_h^u satisfies, for $0 \le l \le k_u$, the following approximation property:

$$\exists C_\kappa > 0 \mid \qquad \|\kappa_h^u q\|_{0,M} \le C_\kappa \frac{h_M^l}{k_u^l}|q|_{l,M}, \quad \forall q\in H^l(M),\ \forall M\in\mathcal{M}_h. \tag{2.7}$$

Due to the consistency of the κ_h^p-dependent stabilization term, thus involving the space D_h^p, we do not need such a condition for D_h^p. In Section 3.5 several choices for the discrete spaces will be presented. For the analysis, the following properties of the stabilization term (2.6) are required.

LEMMA 2.6. *There holds for all* $U,V\in \boldsymbol{V}\times[Q\cap H^1(\Omega)]$

$$(i)\ |S_h(U,V)| \le S_h(U,U)^{\frac12}\ S_h(V,V)^{\frac12}, \tag{2.8}$$

$$(ii)\ S_h(U,U)\ge 0, \tag{2.9}$$

$$(iii)\ S_h(U,U) \le C_S|\boldsymbol{u}|_1^2 + C_\kappa^2\left(\max_{M\in\mathcal{M}_h}\alpha_M\right)|p|_1^2, \quad U=(\boldsymbol{u},p), \tag{2.10}$$

with $C_S := C_\kappa^2 \max_{M\in\mathcal{M}_h}\left[\tau_M\|\boldsymbol{b}\|^2_{(L^\infty(M))^d}+\mu_M\right]$.

Proof. Property (ii) is trivial and (i) follows from the Cauchy-Schwarz inequality. Inequality (iii) can be derived from

$$S_h(U,U)\le C_\kappa^2\sum_{M\in\mathcal{M}_h}\left[\tau_M\|\boldsymbol{b}\|^2_{(L^\infty(M))^d}|u|^2_{1,M}+\mu_M|u|^2_{1,M}+\alpha_M|p|^2_{1,M}\right],$$

using Assumption 2.5 with $l=0$ for the fluctuation operator. □

2.3. Special interpolation operator. Following [21], we construct a special interpolant $j_h^u: H^1(\Omega)\to Y_h$ for the velocity, such that the error $v-j_h^u v$ is L^2-orthogonal to D_h^u for all $v\in H_0^1(\Omega)$. In order to conserve the standard approximation properties, let us suppose the following.

ASSUMPTION 2.7. There exists a constant $\beta_u>0$ (possibly depending on k_u), such that

$$\inf_{q_h\in D_h^u}\ \sup_{v_h\in Y_{h,k_u}(M)} \frac{(v_h,q_h)_M}{\|v_h\|_{0,M}\|q_h\|_{0,M}} \ge \beta_u>0, \tag{2.11}$$

where $Y_{h,k_u}(M) := \{v_h|_M \mid v_h\in Y_{h,k_u}, v_h=0 \text{ on } \Omega\setminus M\}$.

REMARK 2.8. The space D_h^u must not be too rich, since the inf-sup condition (2.11) has to be satisfied. On the other hand, D_h^u must be rich enough to fulfill the approximation property (2.7) . Later on, we will present several function spaces D_h^u which satisfy (2.11).

ETNA
Kent State University
etna@mcs.kent.edu

In the following, we use the notation $a \lesssim b$, if there exists a constant $C > 0$ independent of all relevant sizes, such as mesh size, polynomial degree or coefficients, such that $a \leq Cb$.

LEMMA 2.9. *Let Assumption 2.7 be satisfied. Then there are interpolation operators $j_h^u : H_0^1(\Omega) \to Y_h$ and $\boldsymbol{j}_h^u : \boldsymbol{V} \to \boldsymbol{V}_{h,k_u}$, such that*

$$(v - j_h^u v, q_h)_\Omega = 0, \quad \forall q_h \in D_h^u, \forall v \in H_0^1(\Omega), \tag{2.12}$$

$$\|v - j_h^u v\|_{0,M} + \frac{h_M}{k_u^2}|v - j_h^u v|_{1,M} \lesssim \left(1 + \frac{1}{\beta_u}\right) \frac{h_M^l}{k_u^l}\|v\|_{l,\omega_M}, \tag{2.13}$$

for all $v \in H^l(\Omega) \cap H_0^1(\Omega)$ and

$$(\boldsymbol{v} - \boldsymbol{j}_h^u \boldsymbol{v}, \boldsymbol{q}_h)_\Omega = 0, \quad \forall \boldsymbol{q}_h \in [D_h^u]^d, \ \forall \boldsymbol{v} \in \boldsymbol{V}, \tag{2.14}$$

$$\|\boldsymbol{v} - \boldsymbol{j}_h^u \boldsymbol{v}\|_{0,M} + \frac{h_M}{k_u^2}|\boldsymbol{v} - \boldsymbol{j}_h^u \boldsymbol{v}|_{1,M} \lesssim \left(1 + \frac{1}{\beta_u}\right) \frac{h_M^l}{k_u^l}\|\boldsymbol{v}\|_{l,\omega_M}, \tag{2.15}$$

for all $\boldsymbol{v} \in [H^l(\Omega)]^d \cap \boldsymbol{V}$, $M \in \mathcal{M}_h$, and $1 \leq l \leq k_u + 1$. Here $\omega_M := \bigcup_{T \subset M} \omega_T$ is a neighborhood of $M \in \mathcal{M}_h$.

For better readability, we put the proof in the Appendix. Analogously, a corresponding result can be proved for the pressure.

LEMMA 2.10. *Suppose that there exists a constant $\beta_p > 0$ (possibly depending on k_p), such that*

$$\inf_{q_h \in D_h^p} \sup_{v_h \in Q_{h,k_p}(M)} \frac{(v_h, q_h)_M}{\|v_h\|_{0,M}\|q_h\|_{0,M}} \geq \beta_p. \tag{2.16}$$

Then there exists an interpolation operator $j_h^p : Q \to Q_{h,k_p}$, such that

$$(v - j_h^p v, q_h)_\Omega = 0, \qquad \forall q_h \in D_h^p, \tag{2.17}$$

$$\|v - j_h^p v\|_{0,M} + \frac{h_M}{k_p^2}|v - j_h^p v|_{1,M} \lesssim \left(1 + \frac{1}{\beta_p}\right) \frac{h_M^l}{k_p^l}\|v\|_{l,\omega_M}, \ \ \forall v \in Q \cap H^l(\Omega). \tag{2.18}$$

REMARK 2.11. The estimates of Lemmas 2.9 and 2.10 are optimal with respect to h_M. The estimates in the norm $|\cdot|_{1,M}$ are seemingly sub-optimal regarding to k_u and k_p.

3. A priori analysis.

The next goal is an error estimate for the scheme (2.5). Therefore, further assumptions on the finite element spaces $\boldsymbol{V}_{h,k_u}$, $\boldsymbol{D}_{h,k_u}$, Q_{h,k_p} and D_{h,k_p} are required.

3.1. Stability.

First, the stability of the scheme will be shown. The standard approach is to provide this in the mesh-dependent norm

$$|||V||| := \left(|[V]|^2 + \delta\|q\|_0^2\right)^{\frac{1}{2}}, \quad |[V]|^2 := \|\nu^{\frac{1}{2}}\nabla \boldsymbol{v}\|_0^2 + \|\sigma^{\frac{1}{2}}\boldsymbol{v}\|_0^2 + S_h(V,V),$$

for $V = (\boldsymbol{v}, q) \in \boldsymbol{V} \times Q$ with suitable $\delta > 0$. Here we prefer a separated approach for velocity and pressure by using first the $|[\cdot]|$ semi-norm and then a post-processing argument for the pressure.

LEMMA 3.1. *The following a-priori estimate is valid*

$$\|\nu^{\frac{1}{2}}\nabla \boldsymbol{u}_h\|_0^2 + \|\sigma^{\frac{1}{2}}\boldsymbol{u}_h\|_0^2 \leq |[U_h]|^2 \leq (\boldsymbol{f}, \boldsymbol{u}_h)_\Omega. \tag{3.1}$$

Hence, uniqueness and existence of $\boldsymbol{u}_h \in \boldsymbol{V}_{h,k_u}$ in the scheme (2.5) follows.

ETNA
Kent State University
etna@mcs.kent.edu

Proof. Integration by parts yields $((\boldsymbol{b}\cdot\nabla)\boldsymbol{u}_h,\boldsymbol{u}_h)_\Omega = -\frac{1}{2}((\nabla\cdot\boldsymbol{b})\boldsymbol{u}_h,\boldsymbol{u}_h)_\Omega = 0$, and therefore

$$(A+S_h)(U_h,U_h) = \|\nu^{\frac{1}{2}}\nabla\boldsymbol{u}_h\|_0^2 + \|\sigma^{\frac{1}{2}}\boldsymbol{u}_h\|_0^2 + S_h(U_h,U_h) = |[U_h]|^2. \tag{3.2}$$

This implies (3.1), hence uniqueness and existence of the discrete velocity field $\boldsymbol{u}_h \in \boldsymbol{V}_{h,k_u}$ of the scheme (2.5). □

The corresponding result for the pressure $p_h \in Q_{h,k_p}$ follows from Lemma 3.2 and Lemma 3.1. Here, we use the notation $\nu_\infty = \|\nu\|_{L^\infty(\Omega)}$, $\nu_0 = \inf_\Omega \nu(x)$, $\boldsymbol{b}_\infty = \|\boldsymbol{b}\|_{(L^\infty(\Omega))^d}$.

LEMMA 3.2. *There exists a constant $\gamma > 0$ dependent on the continuous inf-sup constant β and on the polynomial degree k_u but independent of the mesh size h, such that*

$$\|p_h\|_0 \le \gamma\Big(\sqrt{\nu_\infty} + \sqrt{C_P\sigma} + \frac{C_P\boldsymbol{b}_\infty}{\sqrt{\nu_0+\sigma C_P^2}} + \sqrt{C_S} + C_T\Big)|[U_h]| \, + \frac{1}{\beta}\|\boldsymbol{f}\|_{-1}, \tag{3.3}$$

where $C_S = C_\kappa^2 \max_{M\in\mathcal{M}_h}\Big[\tau_M\|\boldsymbol{b}\|^2_{(L^\infty(M))^d} + \mu_M\Big]$ and $C_T = \frac{1}{\beta}\max_M \frac{C_\kappa h_M}{k_u\sqrt{\alpha_M}}$. C_P is the constant in the Poincaré inequality.

Proof. Using the closed range theorem, the continuous inf-sup condition yields the existence of $\boldsymbol{v} \in [H_0^1(\Omega)]^d$ with $\nabla\cdot\boldsymbol{v} = -p_h$ and $|\boldsymbol{v}|_1 \le \frac{1}{\beta}\|p_h\|_0$. We set $\boldsymbol{v}_h := \boldsymbol{j}_h^u\boldsymbol{v}$. Lemma 2.9 together with the triangle inequality imply

$$|\boldsymbol{v}_h|_1 \;\le\; |\boldsymbol{v}|_1 + C\Big(1+\frac{1}{\beta_u}\Big)k_u|\boldsymbol{v}|_1 \le \frac{1}{\beta}\Big[1 + C\Big(1+\frac{1}{\beta_u}\Big)k_u\Big]\|p_h\|_0 \;=:\; C_A\|p_h\|_0.$$

Consider now

$$(\boldsymbol{f},\boldsymbol{v}_h)_\Omega = (A+S_h)(U_h,(\boldsymbol{v}_h,0)) = -(p_h,\nabla\cdot\boldsymbol{v})_\Omega - \sum_{i=1}^3 T_i = \|p_h\|_0^2 - \sum_{i=1}^3 T_i, \tag{3.4}$$

with terms T_i given below. Standard inequalities and integration by parts imply

$$\begin{aligned} T_1 &= (\nu\nabla\boldsymbol{u}_h,\nabla\boldsymbol{v}_h)_\Omega + (\sigma\boldsymbol{u}_h,\boldsymbol{v}_h)_\Omega + ((\boldsymbol{b}\cdot\nabla)\boldsymbol{u}_h,\boldsymbol{v}_h)_\Omega \\ &\le \Big(\nu_\infty^{\frac{1}{2}} + (\sigma C_P)^{\frac{1}{2}} + \frac{C_P\boldsymbol{b}_\infty}{\sqrt{\nu_0+\sigma C_P^2}}\Big)\Big(\|\nu^{\frac{1}{2}}\nabla\boldsymbol{u}_h\|_0^2 + \|\sqrt{\sigma}\boldsymbol{u}_h\|_0^2\Big)^{\frac{1}{2}}|\boldsymbol{v}_h|_1 \\ &\le \Big(\nu_\infty^{\frac{1}{2}} + (\sigma C_P)^{\frac{1}{2}} + \frac{C_P\boldsymbol{b}_\infty}{\sqrt{\nu_0+\sigma C_P^2}}\Big)C_A|[U_h]|\;\|p_h\|_0, \end{aligned}$$

where C_P stems from the Poincaré inequality $\|\boldsymbol{v}_h\|_0 \le C_P^{\frac{1}{2}}|\boldsymbol{v}_h|_1$. Lemma 2.6 gives

$$\begin{aligned} T_2 &= S_h(U_h,(\boldsymbol{v}_h,0)) \le S_h(U_h,U_h)^{\frac{1}{2}}S_h((\boldsymbol{v}_h,0),(\boldsymbol{v}_h,0))^{\frac{1}{2}} \\ &\le \sqrt{C_S}\;|[U_h]|\;|\boldsymbol{v}_h|_1 \;\le\; \sqrt{C_S}C_A\;|[U_h]|\;\|p_h\|_0. \end{aligned}$$

Integration by parts (for continuous discrete pressure space) and Lemma 2.9 yield

$$\begin{aligned} T_3 &= |(\nabla\cdot(\boldsymbol{v}_h-\boldsymbol{v}),p_h)_\Omega| = |(\boldsymbol{v}_h-\boldsymbol{v},\nabla p_h)_\Omega| = |(\boldsymbol{v}_h-\boldsymbol{v},\kappa_h^u\nabla p_h)_\Omega| \\ &\le \Bigg(\sum_M \frac{C_\kappa^2 h_M^2}{k_u^2\alpha_M}|\boldsymbol{v}|_{1,M}^2\Bigg)^{\frac{1}{2}}\;|[U_h]| \;\le\; \frac{1}{\beta}\max_M\frac{C_\kappa h_M}{k_u\sqrt{\alpha_M}}\;|[U_h]|\;\|p_h\|_0. \end{aligned}$$

Furthermore, there holds $(-\boldsymbol{f}, \boldsymbol{v}_h)_\Omega \le \|\boldsymbol{f}\|_{-1}|\boldsymbol{v}_h|_1$ with the norm $\|\cdot\|_{-1}$ in $[H^{-1}(\Omega)]^d$. Using all these estimates, we obtain from (3.4),

$$\|p_h\|_0 \le \left(C_A\left[\sqrt{\nu_\infty} + \sqrt{C_P\sigma} + \frac{C_P \boldsymbol{b}_\infty}{\sqrt{\nu_0 + \sigma C_P^2}} + \sqrt{C_S}\right] + C_T\right)|[U_h]| + C_A\|\boldsymbol{f}\|_{-1}, \tag{3.5}$$

where $C_T := \frac{1}{\beta}\max_M \frac{C_\kappa h_M}{k_u\sqrt{\alpha_M}}$. □

3.2. Approximate Galerkin orthogonality. In LPS methods the Galerkin orthogonality is not fulfilled and a careful analysis of the consistency error has to be done.

LEMMA 3.3. *Let $U \in \boldsymbol{V} \times Q$ and $U_h \in \boldsymbol{V}_{h,k_u} \times Q_{h,k_p}$ be the solutions of (2.1) and of (2.5), respectively. Then, there holds*

$$(A + S_h)(U - U_h, V_h) = S_h(U, V_h), \qquad \forall V_h \in \boldsymbol{V}_{h,k_u} \times Q_{h,k_p}. \tag{3.6}$$

Proof. The assertion (3.6) follows by subtracting (2.5) from (2.1). □

Now the consistency error can be estimated with the help of Lemma 2.6.

LEMMA 3.4. *Let Assumption 2.5 be fulfilled and $(u,p) \in \boldsymbol{V} \times Q$ with $(\boldsymbol{b}\cdot\nabla)\boldsymbol{u} \in (H^{l_u+1}(M))^d$, $\nabla\cdot\boldsymbol{u} = 0$, $p \in H^{l_p+1}(M)$ for all $M \in \mathcal{M}_h$. Then, we obtain for $0 \le l_u, l_p \le k_u$,*

$$|S_h(U, V_h)| \lesssim \left(\sum_{M\in\mathcal{M}_h} \tau_M \frac{h_M^{2l_u}}{k_u^{2l_u}}|(\boldsymbol{b}\cdot\nabla)\boldsymbol{u}|^2_{l_u,M} + \alpha_M \frac{h_M^{2l_p}}{k_p^{2l_p}}|p|^2_{l_p+1,M}\right)^{\frac{1}{2}}|[V_h]|. \tag{3.7}$$

Proof. Lemma 2.6 yields

$$S_h(U, V_h) \le S_h(U,U)^{\frac{1}{2}} S_h(V_h,V_h)^{\frac{1}{2}} \le S_h(U,U)^{\frac{1}{2}}|[V_h]|.$$

Assumption 2.5 and $\nabla\cdot\boldsymbol{u} = 0$ imply

$$S_h(U,U) \lesssim \sum_{M\in\mathcal{M}_h} \tau_M \frac{h_M^{2l_u}}{k_u^{2l_u}}|(\boldsymbol{b}\cdot\nabla)\boldsymbol{u}|^2_{l_u,M} + \alpha_M \frac{h_M^{2l_p}}{k_p^{2l_p}}|p|^2_{l_p+1,M}.$$

Now the assertion follows from these estimates. □

3.3. A priori error estimate. The a priori estimate can be shown by using the standard technique of combining the stability and the consistency results of the last subsections.

THEOREM 3.5. *Let $U = (\boldsymbol{u}, p) \in \boldsymbol{V} \times Q$ be the continuous solution of (2.1) and $U_h = (\boldsymbol{u}_h, p_h) \in \boldsymbol{V}_{h,k_u} \times Q_{h,k_p}$ the discrete solution of (2.5). We assume that the solution $U = (\boldsymbol{u}, p) \in \boldsymbol{V} \times Q$ is sufficiently regular, i.e., $p \in H^{l_p+1}(\Omega)$, $\boldsymbol{u} \in [H^{l_u+1}(\Omega)]^d$, and $(\boldsymbol{b}\cdot\nabla)\boldsymbol{u} \in [H^{l_u}(\Omega)]^d$. Furthermore, let the Assumptions 2.5 and 2.7 for the coarse velocity space D_h^u be satisfied. For the space D_h^p we assume that (2.16) is satisfied. Then, there holds for $1 \le l_u \le k_u$ and $1 \le l_p \le \min\{k_p, k_u\}$,*

$$\begin{aligned} |[U - U_h]|^2 \lesssim \sum_{M\in\mathcal{M}_h} \Bigg(&\tau_M \frac{h_M^{2l_u}}{k_u^{2l_u}}\|(\boldsymbol{b}\cdot\nabla)\boldsymbol{u}\|^2_{l_u,\omega_M} \\ &+ \left(1 + \frac{1}{\beta_u}\right)^2 \frac{h_M^{2l_u}}{k_u^{2l_u-2}} C_M^u\|\boldsymbol{u}\|^2_{l_u+1,\omega_M} + \left(1 + \frac{1}{\beta_p}\right)^2 \frac{h_M^{2l_p}}{k_p^{2l_p-2}} C_M^p\|p\|^2_{l_p+1,\omega_M}\Bigg), \end{aligned} \tag{3.8}$$

ETNA
Kent State University
etna@mcs.kent.edu

where

$$\begin{aligned} C_M^u &:= \|\nu\|_{L^\infty(M)} + \frac{h_M^2}{k_u^4}(\sigma + \frac{1}{\tau_M} + \frac{1}{\alpha_M}) + \mu_M + \|\boldsymbol{b}\|^2_{(L^\infty(M))^d}\tau_M, \\ C_M^p &:= \alpha_M + \frac{1}{\mu_M}\frac{h_M^2}{k_p^4}. \end{aligned}$$

Proof. The error is split into two parts

$$U - U_h = (\boldsymbol{u} - \boldsymbol{u}_h, p - p_h) = (\boldsymbol{u} - \boldsymbol{j}_h^u\boldsymbol{u}, p - j_h^p p) + (\boldsymbol{j}_h^u\boldsymbol{u} - \boldsymbol{u}_h, j_h^p p - p_h).$$

We start with the approximation error $(\boldsymbol{u} - \boldsymbol{j}_h^u\boldsymbol{u}, p - j_h^p p)$. Lemma 2.9 (i) and Lemma 2.10 yield

$$|[(\boldsymbol{u} - \boldsymbol{j}_h^u\boldsymbol{u}, p - j_h^p p)]| \lesssim \left(1 + \frac{1}{\beta_p}\right)\Big(\sum_{M\in\mathcal{M}_h} \frac{h_M^{2l_p}}{k_p^{2l_p-2}}\alpha_M\|p\|^2_{l_p+1,\omega_M}\Big)^{\frac12} \tag{3.9}$$

$$+\left(1 + \frac{1}{\beta_u}\right)\Big(\sum_{M\in\mathcal{M}_h}\Big[\|\nu\|_{L^\infty(M)} + \sigma\frac{h_M^2}{k_u^4} + \mu_M + \tau_M\|\boldsymbol{b}\|^2_{(L^\infty(M))^d}\Big]\frac{h_M^{2l_u}}{k_u^{2l_u-2}}\|\boldsymbol{u}\|^2_{l_u+1,\omega_M}\Big)^{\frac12}.$$

Now we estimate the remaining part $W_h := (\boldsymbol{w}_h, r_h) = (\boldsymbol{j}_h^u\boldsymbol{u} - \boldsymbol{u}_h, j_h^p p - p_h)$ via Lemma 3.1,

$$\begin{aligned} |[(\boldsymbol{j}_h^u\boldsymbol{u} - \boldsymbol{u}_h, j_h^p p - p_h)]| &= \frac{(A + S_h)((\boldsymbol{j}_h^u\boldsymbol{u} - \boldsymbol{u}_h, j_h^p p - p_h), W_h)}{|[W_h]|} \\ &= \underbrace{\frac{(A + S_h)((\boldsymbol{u} - \boldsymbol{u}_h, p - p_h), W_h)}{|[W_h]|}}_{:=I} + \underbrace{\frac{(A + S_h)((\boldsymbol{j}_h^u\boldsymbol{u} - \boldsymbol{u}, j_h^p p - p), W_h)}{|[W_h]|}}_{=:II}. \end{aligned}$$

Applying Lemmas 3.3 and 3.4, the first term is bounded by

$$I = \frac{S_h((\boldsymbol{u}, p), W_h)}{|[W_h]|} \lesssim \sum_{M\in\mathcal{M}_h}\left(\tau_M\frac{h_M^{2l_u}}{k_u^{2l_u}}\|(\boldsymbol{b}\cdot\nabla)\boldsymbol{u}\|^2_{l_u,M} + \alpha_M\frac{h_M^{2l_p}}{k_p^{2l_p}}\|p\|^2_{l_p+1,M}\right)^{\frac12}.$$

Now we consider the terms of II separately. Integration by parts and property (2.14) yield

$$\begin{aligned} &(\nu\nabla(\boldsymbol{j}_h^u\boldsymbol{u} - \boldsymbol{u}), \nabla\boldsymbol{w}_h)_\Omega + (\sigma(\boldsymbol{j}_h^u\boldsymbol{u} - \boldsymbol{u}), \boldsymbol{w}_h)_\Omega + ((\boldsymbol{b}\cdot\nabla)(\boldsymbol{j}_h^u\boldsymbol{u} - \boldsymbol{u}), \boldsymbol{w}_h)_\Omega \\ &= (\nu\nabla(\boldsymbol{j}_h^u\boldsymbol{u} - \boldsymbol{u}), \nabla\boldsymbol{w}_h)_\Omega + (\sigma(\boldsymbol{j}_h^u\boldsymbol{u} - \boldsymbol{u}), \boldsymbol{w}_h)_\Omega - (\boldsymbol{\kappa}_h^u((\boldsymbol{b}\cdot\nabla)\boldsymbol{w}_h), \boldsymbol{j}_h^u\boldsymbol{u} - \boldsymbol{u})_\Omega \\ &\lesssim \left(1 + \frac{1}{\beta_u}\right)\Big(\sum_{M\in\mathcal{M}_h}\frac{h_M^{2l_u}}{k_u^{2l_u-2}}\left[\|\nu\|_{L^\infty(M)} + (\sigma + \frac{1}{\tau_M})\frac{h_M^2}{k_u^4}\right]\|\boldsymbol{u}\|^2_{l_u+1,\omega_M}\Big)^{\frac12}|[W_h]|. \end{aligned}$$

The orthogonality property (2.14) results in

$$\begin{aligned} |(p - j_h^p p, \nabla\cdot\boldsymbol{w}_h)_\Omega| &= |(p - j_h^p p, \kappa_h^p\nabla\cdot\boldsymbol{w}_h)_\Omega| \\ &\lesssim \left(1 + \frac{1}{\beta_p}\right)\Big(\sum_{M\in\mathcal{M}_h}\frac{h_M^{2l_p+2}}{k_p^{2l_p+2}}\mu_M^{-1}\|p\|^2_{l_p+1,\omega_M}\Big)^{\frac12}|[W_h]|. \end{aligned}$$

Integration by parts (due to continuous discrete pressure) and (2.14) lead to

$$|(r_h, \nabla\cdot(\boldsymbol{j}_h^u\boldsymbol{u} - \boldsymbol{u}))_\Omega| \le |(\nabla r_h, \boldsymbol{j}_h^u\boldsymbol{u} - \boldsymbol{u})_\Omega| = |\kappa_h^u(\nabla r_h), \boldsymbol{j}_h^u\boldsymbol{u} - \boldsymbol{u})_\Omega| \tag{3.10}$$

$$\lesssim \left(1 + \frac{1}{\beta_u}\right)\Big(\sum_{M\in\mathcal{M}_h}\frac{1}{\alpha_M}\frac{h_M^{2l_u+2}}{k_u^{2l_u+2}}\|\boldsymbol{u}\|^2_{l_u+1,\omega_M}\Big)^{\frac12}|[W_h]|.$$

The estimation of the stabilization term is straightforward

$$
\begin{aligned}
&|S_h((\boldsymbol{j}_h^u\boldsymbol{u}-\boldsymbol{u}, j_h^p p - p), W_h)\\
&\leq \left(S_h((\boldsymbol{j}_h^u\boldsymbol{u}-\boldsymbol{u}, j_h^p p - p),(\boldsymbol{j}_h^u\boldsymbol{u}-\boldsymbol{u}, j_h^p p - p)\right)^{\frac{1}{2}} \left(S_h(W_h,W_h)\right)^{\frac{1}{2}}\\
&\lesssim \left(1+\frac{1}{\beta_u}\right)\Big(\sum_{M\in\mathcal{M}_h}\frac{h_M^{2l_u}}{k_u^{2l_u-2}}\left[\tau_M\|\boldsymbol{b}\|^2_{(L^\infty(M))^d}+\mu_M\right]\|\boldsymbol{u}\|^2_{l_u+1,\omega_M}\Big)^{\frac{1}{2}}|[W_h]|\\
&\quad+\left(1+\frac{1}{\beta_p}\right)\Big(\sum_{M\in\mathcal{M}_h}\alpha_M\frac{h_M^{2l_p}}{k_p^{2l_p-2}}\|p\|^2_{l_p+1,\omega_M}\Big)^{\frac{1}{2}}|[W_h]|.
\end{aligned}
$$

Adding up all inequalities for the estimate of $|[W_h]|^2 = I + II$ together with the estimate of (3.9) gives the assertion. ∎

COROLLARY 3.6. *Under the assumptions of Theorem 3.5 and the notation of Lemma 3.2, we obtain*

$$
\|p-p_h\|_0 \lesssim \gamma\Big(\sqrt{\nu_\infty}+\sqrt{C_P\sigma}+\min\big(\frac{C_P}{\sqrt{\nu_0}};\frac{1}{\sqrt{\sigma}}\big)\boldsymbol{b}_\infty+\frac{\sqrt{C_S}}{\beta}+C_T\Big)|[U-U_h]|, \tag{3.11}
$$

with constants γ, C_S, C_T and β as in Lemma 3.2.

Proof. The proof mimics the proof of Lemma 3.2. In equation (3.4), one has to replace $U_h = (u_h, p_h)$ by $U - U_h = (\boldsymbol{u}-\boldsymbol{u}_h, p-p_h)$ and $(f, \boldsymbol{v}_h)_\Omega$ by $S_h(U-U_h, (j_h^u\boldsymbol{v}, 0))$. ∎

3.4. Parameter design. Now we will calibrate the stabilization parameters α_M, τ_M, and μ_M with respect to the local mesh size h_M, the polynomial degrees k_u and k_p of the discrete ansatz functions and problem data. The parameters are determined by minimizing and balancing the terms of the right-hand side of the general a priori error estimation.

First, equilibrating the τ_M-dependent terms in C_M^u yields

$$
\tau_M \sim \frac{h_M}{\|\boldsymbol{b}\|_{(L^\infty(M))^d}k_u^2}. \tag{3.12}
$$

Similarly, equilibration of the terms in C_M^u and C_M^p involving μ_M and α_M yields

$$
\mu_M \sim \frac{h_M^{l_p-l_u+1}}{k^{l_p-l_u+2}}, \qquad \alpha_M \sim \frac{h_M^{l_u-l_p+1}}{k^{l_u-l_p+2}}, \tag{3.13}
$$

where we used $k \sim k_u \sim k_p$. For the following result, we assume that the solution (u, p) of the continuous Oseen problem is sufficiently smooth.

COROLLARY 3.7. *For equal-order interpolation $k = k_u = k_p \geq 1$, let $l = l_u = l_p \leq k$ and*

$$
\mu_M = \frac{\mu_0 h_M}{k^2}, \qquad \alpha_M = \frac{\alpha_0 h_M}{k^2}, \qquad \tau_M = \frac{\tau_0 h_M}{\|\boldsymbol{b}\|_{(L^\infty(M))^d}k^2}. \tag{3.14}
$$

Then we obtain, under assumptions of Theorem 3.5,

$$
\begin{aligned}
|[U-U_h]|^2 \lesssim \sum_{M\in\mathcal{M}}\Big(&\Big(1+\frac{1}{\beta_p}\Big)^2\frac{h_M^{2l+1}}{k^{2l}}\|p\|^2_{l+1,\omega_M}+\frac{h_M^{2l+1}}{k^{2l+2}}\|(\frac{\boldsymbol{b}}{\|\boldsymbol{b}\|_{(L^\infty(M))^d}}\cdot\nabla)\boldsymbol{u}\|^2_{l,\omega_M}\\
&+\Big(1+\frac{1}{\beta_u}\Big)^2\left[\|\nu\|_{L^\infty(M)}+\sigma\frac{h_M^2}{k^4}+\|\boldsymbol{b}\|_{(L^\infty(M))^d}\frac{h_M}{k^2}\right]\frac{h_M^{2l}}{k^{2l-2}}\|\boldsymbol{u}\|^2_{l+1,\omega_M}\Big).
\end{aligned}
$$

For inf-sup stable interpolation with $k_u = k_p + 1$, we assume $l_u = l_p + 1 = k_u$ and set

$$\alpha_M = \frac{\alpha_0 h_M^2}{k_u^3}, \quad \mu_M = \frac{\mu_0}{k_u}, \quad \tau_M = \frac{\tau_0 h_M}{\|\boldsymbol{b}\|_{(L^\infty(M))^d} k_u^2}. \tag{3.15}$$

Then we obtain, under assumptions of Theorem 3.5,

$$\begin{aligned} |||[U - U_h]|^2 \lesssim \sum_{M\in\mathcal{M}} \Bigg(\left(1 + \frac{1}{\beta_p}\right)^2 \frac{h_M^{2l_u}}{k_u^{2l_u+1}} \|p\|^2_{l_u,\omega_M} + \frac{h_M^{2l_u+1}}{k_u^{2l_u+2}} \|(\frac{\boldsymbol{b}}{\|\boldsymbol{b}\|_{(L^\infty(M))^d}} \cdot \nabla)\boldsymbol{u}\|^2_{l,\omega_M} \\ + \left(1 + \frac{1}{\beta_u}\right)^2 \left[\|\nu\|_{L^\infty(M)} + \sigma \frac{h_M^2}{k_u^4} + \|\boldsymbol{b}\|_{(L^\infty(M))^d} \frac{h_M}{k_u^2} + \frac{1}{k_u} \right] \frac{h_M^{2l_u}}{k_u^{2l_u-2}} \|\boldsymbol{u}\|^2_{l+1,\omega_M} \Bigg). \end{aligned}$$

This result requires some further discussion:

- For equal-order pairs $V_{h,k} \times Q_{h,k}$ and for (inf-sup stable) Taylor-Hood pairs $V_{h,k+1} \times Q_{h,k}$, we obtain the optimal convergence rates $\mathcal{O}(h_M^{k+\frac{1}{2}})$ and $\mathcal{O}(h_M^{k+1})$, respectively, with respect to h_M.
- Due to the non-optimal convergence order of the interpolation operators $\boldsymbol{j}_h^u, j_h^p$ in the $|\cdot|_1$-norm, these estimates are presumably not optimal with respect to polynomial degree k_u. Let us assume that in Lemma 2.9 there holds

$$\frac{h_M}{k_u}|v - j_h^u v|_{1,M} \lesssim \left(1 + \frac{1}{\beta_u}\right) \frac{h_M^l}{k^l} \|v\|_{l,\omega_M} \tag{3.16}$$

  and a similar result in Lemma 2.10 as well. A careful check of the proofs leads to

$$\mu_M = \mu_0 \frac{h_M}{k}, \quad \alpha_M = \alpha_0 \frac{h_M}{k}, \qquad \tau_M = \tau_0 \frac{h_M}{\|\boldsymbol{b}\|_{(L^\infty(\Omega))^d} k_u} \tag{3.17}$$

  for equal-order pairs with $k = k_u = k_p$ and

$$\alpha_M = \alpha_0 \frac{h_M^2}{k_u^2}, \qquad \mu_M = \mu_0 \sim 1, \qquad \tau_M = \tau_0 \frac{h_M}{\|\boldsymbol{b}\|_{(L^\infty(\Omega))^d} k_u} \tag{3.18}$$

  for inf-sup stable pairs with $k_u = k_p + 1$. Then the a-priori estimate (3.8) in Theorem 3.5 would be optimal with respect to k_u and k_p, too, with the possible exception of the factors depending on β_u and β_p. The latter reason eventually leads to a non-optimal parameter design with respect to k_u.
- The formulas for the stabilization parameters and the error estimates are only asymptotic statements. To the best of our knowledge, there is so far no general concept for a more precise design of the stabilization parameters (with the possible exception of one-dimensional problems with constant coefficients). Unfortunately, this leaves the practitioner with the problem of choosing τ_0, ν_0, α_0. Table 4.1 below might give an indication of suitable values in our experiments for an academic problem.

REMARK 3.8. The SUPG parameter τ_M in residual-based stabilization methods has the typical design $\tau_M \sim \min\left(\frac{h_M}{\|\boldsymbol{b}\|_{(L^\infty(M))^d)} k_u}; \frac{1}{\sigma}; \frac{h_M^2}{k_u^2 \nu}\right)$; see [20]. This can be rewritten as $\tau_M \sim \min\left(\frac{h_M^2}{\nu k_u^2} \min\left(1; \frac{1}{Re_M}\right); \frac{1}{\sigma}\right)$ with the local Reynolds number $Re_M = \frac{h_M \|\boldsymbol{b}\|_{[L^\infty(M)]^d)}}{k_u \nu}$. This means that the design of the SUPG-like parameter τ_M in (3.17)-(3.18) is strongly simplified for the LPS method due to the symmetric stabilization term S_h. This choice will not cause problems for locally vanishing $\mathbf{b}$ as the corresponding stabilization term is $\sum_M \tau_M(\kappa_h^u((\mathbf{b}\cdot\nabla)\mathbf{u}_h, \kappa_h^u((\mathbf{b}\cdot\nabla)\mathbf{v}_h))_M$. Clearly, a proper implementation is required. In the Stokes limit $\mathbf{b}=\mathbf{0}$, the SUPG-type stabilization term given above does not occur, hence $\tau_M = 0$. Regarding the remaining stabilization terms, the PSPG-type term can be omitted for inf-sup stable elements. As a consequence, no suboptimality occurs in the analysis for the Stokes limit.

REMARK 3.9. The corresponding result for the LPS scheme with local projection of the full velocity gradient, see Remark 2.4, leads to the design $\delta_M \sim h_M/k_u^2$ (or $\delta_M \sim h_M/k_u$). Please note that the error estimates deteriorate if the local projection of the divergence terms is omitted. Then, the critical term in the proof of Theorem 3.5 is $|(p - j_h^p p, \nabla\cdot \boldsymbol{w}_h)_\Omega|$.

3.5. Choice of the discrete spaces. The paper [21] presents different variants for the choice of the discrete spaces $V_{h,k_u}\times Q_{h,k_p}$ and $D_h^u \times D_h^p$ using simplicial and hexahedral elements. There are basically two variants:

- A two-level variant with a suitable refinement $\mathcal{T}_h$ of $\mathcal{M}_h$ (formally denoted by $\mathcal{M}_h = \mathcal{T}_{2h}$).
- A one-level variant with $\mathcal{M}_h = \mathcal{T}_h$, hence $h_M = h_K$, with a proper enrichment of $P_{k_u,\mathcal{T}_h}$ by using bubble functions.

In the numerical results below, we restrict ourselves to the two-level approach, but the theory also covers the one-level approach. Note that the present analysis covers only the case of continuous pressure approximation. For an extension to discontinuous discrete pressure approximation, in particular to the case of $Q_k/P_{-(k-1)}$-elements, we refer to [23].

The discontinuous coarse spaces are defined on the coarser mesh $\mathcal{M}_h$ with polynomials of one degree less. Thus, for hexahedral elements the coarse spaces are given by

$$D_h^u = Q_{k_u-1,\mathcal{M}_h}, \qquad D_h^p = Q_{k_p-1,\mathcal{M}_h}.$$

For simplicial elements we obtain

$$D_h^u = P_{k_u-1,\mathcal{M}_h}, \qquad D_h^p = P_{k_p-1,\mathcal{M}_h}.$$

Obviously, Assumption 2.5 is valid for our discrete spaces if the local L^2-projection π_M^u : $L^2(M) \to D_h^u(M)$ for the velocity and similarly for the pressure is applied; see [21]. Moreover, for these choices the constants $\beta_{u/p}$ in Assumption 2.7 and in (2.16) scale like $\mathcal{O}(1/\sqrt{k_{u/p}})$ for simplicial elements and like $\mathcal{O}(1)$ for quadrilateral elements in the affine linear case; see [23].

4. Numerical results.

4.1. The Oseen problem. A proper calibration of the stabilization parameters requires careful numerical experiments going beyond the scope of this paper. Some papers validate the parameter design and the theoretical convergence rates for the Oseen problem

$$\begin{aligned} L_{Os}(\boldsymbol{u},p) := -\nu\triangle\boldsymbol{u} + (\boldsymbol{b}\cdot\nabla)\boldsymbol{u} + \sigma\boldsymbol{u} + \nabla p = \boldsymbol{f} &\quad \text{in } \Omega,\\ \nabla\cdot\boldsymbol{u} = 0 &\quad \text{in } \Omega, \end{aligned} \tag{4.1}$$

where $\Omega = (0,1)^2$, using the smooth solution

$$\boldsymbol{u}(x_1,x_2) = \big(\sin(\pi x_1), -\pi x_2\cos(\pi x_1)\big), \qquad p(x_1,x_2) = \sin(\pi x_1)\cos(\pi x_2),$$

and $\boldsymbol{b} = \boldsymbol{u}$. The source term $\boldsymbol{f}$ and the Dirichlet data follow from $\boldsymbol{u}$. We refer to a study in [25] of the one-level variant for equal-order pairs with enrichment of the velocity space by using bubble functions. The two-level variant with inf-sup stable pairs can be found in [19] for equal-order and for inf-sup stable pairs; for the latter case, see also [23]. In all these cases, the local L^2-projection is used for the definition of the fluctuation operators $\kappa_h^{u/p}$.

As an example, some typical results are presented for the two-level variant with Q_2/Q_1 and the Q_2/Q_2 pairs on unstructured, quasi-uniform meshes. More precisely, the coarse spaces D_h^u is constructed as discussed in Subsection 2.2. Moreover, we set $D_h^p = \{0\}$, which results in full grad-div-stab stabilization, i.e., $\kappa_h^p = \mathrm{id}$. The results in Table 4.1 with the errors $\boldsymbol{e}_u = \boldsymbol{u} - \boldsymbol{u}_h$ and $e_p = p - p_h$ for the advection-dominated case $\nu = 10^{-6}$ show comparable results for the best variants of Q_2/Q_1 and Q_2/Q_2, although the results for Q_2/Q_2 are slightly better due to the better pressure approximation.

TABLE 4.1
Two-level LPS scheme: Comparison of different variants of stabilization for problem (4.1) with Q_2/Q_1 and Q_2/Q_2 pairs and $\nu = 10^{-6}, \sigma = 1, h = \frac{1}{64}$.

Pair	τ_0	μ_0	α_0	$\lvert\boldsymbol{e}_u\rvert_1$	$\lVert\boldsymbol{e}_u\rVert_0$	$\lVert\nabla\cdot\boldsymbol{u}_h\rVert_0$	$\lVert e_p\rVert_0$
Q_2/Q_1	0.000	0.000	0.000	2.56E-1	5.42E-4	2.02E-1	2.31E-4
	0.056	0.562	0.010	1.91E-3	6.21E-6	1.82E-4	9.08E-5
	0.056	0.562	0.000	1.91E-3	6.20E-6	1.66E-4	8.06E-5
	0.000	0.562	0.000	2.61E-3	7.42E-6	1.72E-4	8.05E-5
	3.162	0.000	0.000	1.87E-2	7.50E-5	1.56E-2	1.08E-4
Q_2/Q_2	0.000	0.000	0.000	2.38E+1	5.35E-2	1.45E+1	1.66E+3
	0.000	0.000	0.018	1.65E-2	3.48E-5	9.37E-3	6.96E-6
	0.056	1.000	0.018	9.30E-4	2.85E-6	2.14E-4	4.31E-6
	0.056	0.000	0.018	1.77E-3	4.18E-6	1.46E-3	3.25E-6
	0.000	5.623	0.018	3.26E-3	7.20E-6	2.00E-4	7.56E-6

Nevertheless, the importance of the stabilization terms is different. The small-scale SUPG- and PSPG-type terms are necessary for the equal-order case but not for the inf-sup stable pair. At least the PSPG-type term can be omitted for the inf-sup stable case. On the other hand, the divergence-stabilization gives clear improvement for the inf-sup stable case and some improvement for the equal-order case. Let us remark that the divergence stabilization without local projection has better algebraic properties than its LPS variant.

In Figure 4.1, convergence plots are shown for the two-level LPS scheme with optimized parameters in the diffusion- and advection-dominated cases with $\nu = 1$ and $\nu = 10^{-6}$, respectively. The numerical convergence rates confirm the theoretical results. Interestingly, no gain of the better pressure approximation for the Q_2/Q_2 pair can be observed in the diffusion-dominated case.

Let us finally check the effect of increasing polynomial degree for inf-sup stable Taylor-Hood pairs Q_r/Q_{r-1} with $r \in \{2,3,4,5\}$. This is shown in Figure 4.2 for $\nu = 10^{-6}, \sigma = 1$, and different values of h. Similar results are obtained (but not shown) for equal-order approximation with Q_r/Q_r-elements with $r \in \{1,2,3,4,5\}$.

4.2. Navier-Stokes problem. Finally, we apply the LPS stabilization to the lid-driven cavity flow as a standard Navier-Stokes benchmark problem (4.1) with $\boldsymbol{b} = \boldsymbol{u}$, $\sigma = 0$ and $\boldsymbol{f} = \boldsymbol{0}$. Homogeneous Dirichlet data are prescribed with the exception of the upper part of the boundary where $\boldsymbol{u} = (1,0)^T$ is given. An unstructured quasi-uniform mesh is used together with the Taylor-Hood pair Q_2/Q_1 and the equal-order Q_2/Q_2 pair using the two-level variant of LPS stabilization with scaling parameter τ_0 and μ_0 according to our theory and $\alpha_0 = 0$. In particular, the cases $\tau_0 = \mu_0 = 0$ correspond to no stabilization.

ETNA
Kent State University
etna@mcs.kent.edu

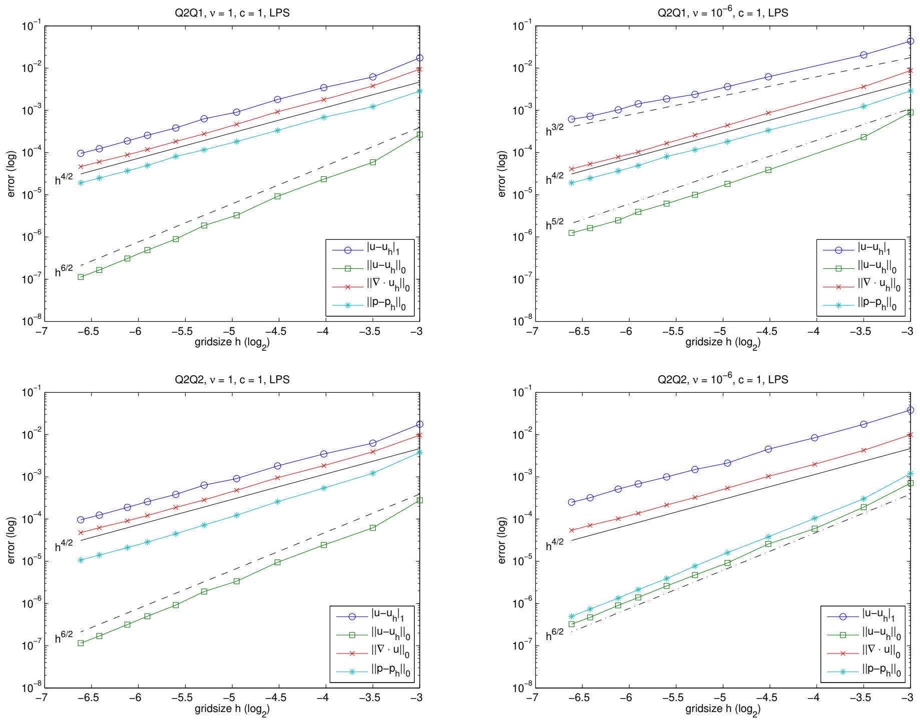

FIG. 4.1. *h-convergence for the Oseen problem with $\nu = 1$ (left) and $\nu = 10^{-6}$ (right) with $\sigma = 1$.*

In Figure 4.3, we present typical solution profiles of the velocity for the case of $Re = 5{,}000$. The results for $h = \frac{1}{64}$ for both variants are in excellent agreement with the reference data in [11], where the stream function-vorticity formulation of the Navier-Stokes problem on very fine meshes with up to 601×601 nodes is used. In particular, the boundary layers are well resolved even on this quasi-uniform mesh. Moreover, the solution for a coarse grid with $h = \frac{1}{16}$ is in good agreement with the data in [11] away from the boundary layers. The results confirm the previous remarks for the linearized problem of Oseen type. For the Q_2/Q_1 element, only the divergence stabilization is necessary whereas for the Q_2/Q_2 pair all stabilization terms are important.

Then, we compare in Table 4.2 the positions and values of extrema of the velocity profiles for different values of Re. The results for the two-level LPS scheme with the Q_2/Q_1 pair on the fine mesh with $h \approx 1/256$ are in good agreement with the results in [3, 27]. Moreover, the LPS results on the coarser grid with $h \approx 1/32$ are in good agreement with the case $h \approx 1/256$. This is verified in h-convergence studies in [19].

Finally, we compare in Table 4.3 the position (x_c, y_c) of the main vortex and the values of the streamfunction Ψ_{mine} and of the vorticity ω_c in the (x_c, y_c). for two values of Re. The results for the two-level LPS scheme with the Q_2/Q_1 pair on the fine mesh with $h \approx 1/256$ are in very good agreement with the results in [3, 11], but slightly different from the results in [27]. Studies of h-convergence can be found in [19].

5. Summary. A unified a-priori analysis of stabilized methods via local projection (LPS) is given for equal-order and inf-sup stable velocity-pressure pairs on isotropic meshes. The error estimates are comparable to classical residual-based stabilized (RBS) methods. This shows that only stabilization of the fine scales is necessary. Compared to the RBS methods,

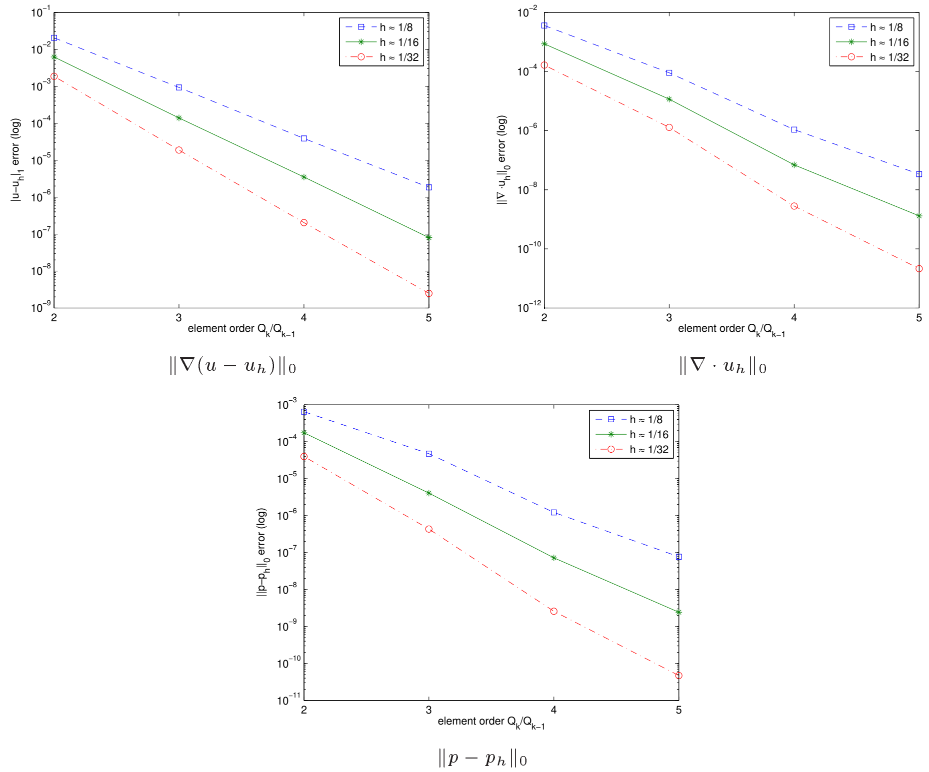

FIG. 4.2. *Polynomial convergence for the Oseen problem with $\nu = 10^{-6}, \sigma = 1$ for fixed h.*

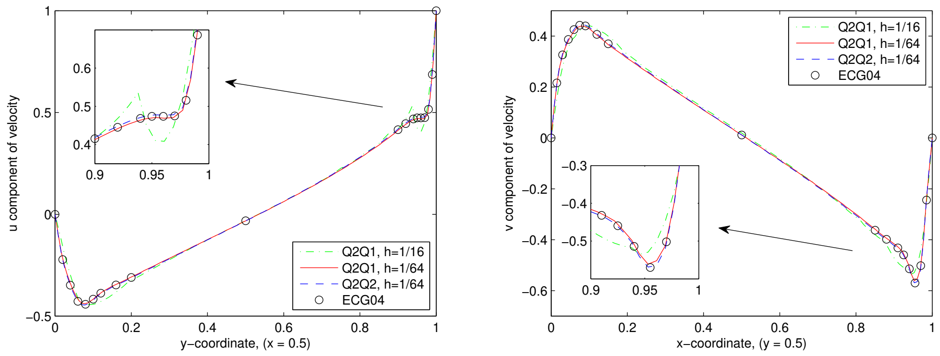

FIG. 4.3. *Lid driven-cavity problem with $Re = 5,000$: Cross-sections of the discrete solutions for Q_2/Q_1 pair with $\tau_0 = \alpha_0 = 0$ and $\mu_0 = 0.562$ and Q_2/Q_2 pair with $\tau_0 = 0.056, \alpha_0 = 0.018, \mu_0 = 1$.*

the design of the stabilization parameters is much simpler for LPS schemes as the strong coupling of velocity and pressure in the stabilization terms does not occur.

Numerical results from the literature and our own experiments confirm both, the design of the stabilization terms and the theoretical convergence rates. A major difference between equal-order pairs and inf-sup stable pairs is that LPS-stabilization is always necessary for equal-order pairs. For inf-sup stable pairs, the necessity of stabilization is seemingly much

ETNA
Kent State University
etna@mcs.kent.edu

TABLE 4.2
Lid driven-cavity problem for different values of Re: Maxima and minima on cross-sections $x = 0.5$ and $y = 0.5$; a) LPS Q_2Q_1, $h \approx 1/32$, b) LPS Q_2Q_1, $h \approx 1/256$, c) $h = 1/256$ (in [12]), d) $h = 1/256$ (in [27]), e) spectral method with $N = 1/160$ (in [3]).

Re		u_{min}	y_{min}	v_{max}	x_{max}	v_{min}	x_{min}
100	a)	−0.21399	0.45703	0.17951	0.23828	−0.25376	0.80859
	b)	−0.21404	0.45703	0.17957	0.23828	−0.25378	0.80859
	d)	−0.21411	0.45898	0.17946	0.23633	−0.25391	0.81055
	e)	−0.21404	0.4581	0.17957	0.2370	−0.25380	0.8104
1000	a)	−0.38512	0.17578	0.37404	0.16016	−0.52295	0.90625
	b)	−0.38857	0.17188	0.37692	0.15625	−0.52701	0.91016
	d)	−0.39009	0.16992	0.37847	0.15820	−0.52839	0.90820
	e)	−0.38857	0.1717	0.37695	0.1578	−0.52708	0.9092
7500	a)	−0.43940	0.07031	0.43749	0.07813	−0.56560	0.96484
	b)	−0.45478	0.06250	0.45836	0.06641	−0.58043	0.96484
	c)	−0.43590	0.0625	0.44030	0.0703	−0.55216	0.9609
	d)	−0.46413	0.06445	0.47129	0.06836	−0.58878	0.96289

TABLE 4.3
Lid driven-cavity problem for different values of Re: Position of center of main vortex and values of stream function Ψ_{min} and of vorticity ω_c; a) LPS Q_2Q_1, $h \approx 1/32$, b) LPS Q_2Q_1, $h \approx 1/256$, c) $h = 1/256$ (in [11]), d) $h = 1/256$ (in [27]), e) spectral method with $N = 1/160$ (in [3]).

Re		Ψ_{min}	ω_c	x_c	y_c
1000	a)	−0.118310	−2.06527	0.5314	0.5676
	b)	−0.118936	−2.06772	0.5308	0.5651
	c)	−0.118942	−2.06721	0.5300	0.5650
	d)	−0.1193	–	0.5313	0.5664
	e)	−0.118937	−2.06775	0.5308	0.5652
7500	a)	−0.119315	−1.86210	0.5192	0.5293
	b)	−0.122386	−1.92691	0.5122	0.5321
	c)	−0.122386	−1.92697	0.5133	0.5317
	d)	−0.1253	–	0.5177	0.5313

less pronounced as for equal-order pairs. In particular, the grad-div stabilization is much more important than the fine-scale SUPG stabilization. Moreover, the fine-scale PSPG part seems to be superfluous.

Appendix.

LEMMA A.1. *Let Assumption 2.7 be satisfied. Then there are interpolation operators $j_h^u : H_0^1(\Omega) \to Y_h$ and $\boldsymbol{j}_h^u : \boldsymbol{V} \to \boldsymbol{V}_{h,k_u}$, such that*

$$(v - j_h^u v, q_h)_\Omega = 0 \;\; \forall q_h \in D_h^u,\; \forall v \in H_0^1(\Omega), \tag{A.1}$$

$$\|v - j_h^u v\|_{0,M} + \frac{h_M}{k_u^2}|v - j_h^u v|_{1,M} \lesssim \left(1 + \frac{1}{\beta_u}\right)\frac{h_M^l}{k_u^l}\|v\|_{l,\omega_M}, \tag{A.2}$$

for all $v \in H^l(\Omega) \cap H_0^1(\Omega)$, and

$$(\boldsymbol{v} - \boldsymbol{j}_h^u \boldsymbol{v}, \boldsymbol{q}_h)_\Omega = 0 \;\; \forall \boldsymbol{q}_h \in [D_h^u]^d,\; \forall \boldsymbol{v} \in \boldsymbol{V}, \tag{A.3}$$

$$\|\boldsymbol{v} - \boldsymbol{j}_h^u \boldsymbol{v}\|_{0,M} + \frac{h_M}{k_u^2}|\boldsymbol{v} - \boldsymbol{j}_h^u \boldsymbol{v}|_{1,M} \lesssim \left(1 + \frac{1}{\beta_u}\right)\frac{h_M^l}{k_u^l}\|\boldsymbol{v}\|_{l,\omega_M}, \tag{A.4}$$

ETNA
Kent State University
etna@mcs.kent.edu

for all $\boldsymbol{v} \in [H^l(\Omega)]^d \cap \boldsymbol{V}$, $M \in \mathcal{M}_h$, *and* $1 \leq l \leq k_u + 1$. *Here* $\omega_M := \bigcup_{T \subset M} \omega_T$ *is a neighborhood of* $M \in \mathcal{M}_h$.

Proof. We follow the lines of the proof of [21, Theorem 2.2], but we take into account the dependency of the constants on the polynomial order and the inf-sup constant β_u.

Define the linear continuous operator $B_h : Y_h(M) \to D_h^u(M)'$ by

$$\langle B_h v_h, q_h \rangle := (v_h, q_h)_M, \qquad \forall v_h \in Y_h(M), q_h \in D_h^u(M).$$

The Closed-Range Theorem yields via Assumption 2.7 that B_h is an isomorphism from $W_h(M)^\perp$ onto $D_h^u(M)'$ with $\beta_u \|v_h\|_{0,M} \leq \|B_h v_h\|_{D_h^u(M)'}, v_h \in W_h(M)^\perp$, where $W_h(M)^\perp$ is the orthogonal complement of $W_h(M) := Ker(B_h)$ with respect to $(\cdot,\cdot)_M$.

Let $M \in \mathcal{M}_h$ and $v \in H_0^1(\Omega)$ be arbitrary. Then, there exists a unique $z_h(v, M) \in W_h(M)^\perp$ with $\|z_h(v,M)\| \leq \frac{1}{\beta}_u \|v - I_{h,k_u} v\|_{0,M}$, such that

$$\langle B_h z_h(v, M), q_h \rangle = (z_h(v), q_h)_M = (v - I_{h,k_u} v, q_h)_M, \quad \forall q_h \in D_h^u(M). \tag{A.5}$$

Now, we define local operators $j_{h,M}^u : H_0^1(\Omega) \to Y_h(M)$, $M \in \mathcal{M}_h$, by $j_{h,M}^u v := (I_{h,k_u}^u v)|_M + z_h(v, M)$. Since $\mathcal{M}_h$ is a partition of Ω, we can define a global operator $j_h^u : H_0^1(\Omega) \to Y_h$ by $(j_h^u v)|_M := j_{h,M}^u v$. Due to (2.3), the operator j_h^u satisfies for $1 \leq l \leq k_u + 1$ and all $T \in \mathcal{T}_h$, $v \in H_0^1(\Omega) \cap H^l(\Omega)$,

$$\|v - j_h^u v\|_{0,M}^2 \leq \left(1 + \frac{1}{\beta_u}\right)^2 \|v - I_{h,k_u}^u v\|_{0,M}^2 \leq C \left(1 + \frac{1}{\beta_u}\right)^2 \sum_{\substack{T \subset M \\ T \in \mathcal{T}_h}} \frac{h_T^{2l}}{k)_u^{2l}} \|v\|_{l,\omega_T}^2. \tag{A.6}$$

The approximation property in the H^1-seminorm follows from inequality (2.2),

$$|z_h(v, M)|_{1,M}^2 \leq \sum_{\substack{T \subset M \\ T \in \mathcal{T}_h}} \mu_{inv} k_u^2 h_T^{-1} \|z_h(v, M)\|_{0,T}^2 \leq \frac{\mu_{inv}^2}{\beta_u} \sum_{\substack{T \subset M \\ T \in \mathcal{T}_h}} k_u^4 h_T^{-2} \|v - I_{h,k_u}^u v\|_{0,T}^2,$$

and using the approximation property (2.3),

$$\begin{aligned} |v - j_h^u v|_{1,M}^2 &= |v - I_{h,k_u}^u v - z_h(v, M)|_{1,M}^2 \leq 2|v - I_{h,k_u}^u v|_{1,M}^2 + 2|z_h(v, M)|_{1,M}^2 \\ &\lesssim \left(\frac{1}{k_u} + \frac{\mu_{inv}}{\beta_u^2}\right) \frac{h_M^{l-1}}{k_u^{l-2}} |v|_{l,\omega_M}. \end{aligned}$$

Finally, the orthogonality property (A.1) is a consequence of (A.5). ☐

REFERENCES

[1] I. BABUŠKA AND M. SURI, *The p and h-p versions of the finite element method, basic principles and properties*, SIAM Rev., 36 (1994), pp. 578–632.
[2] Y. BAZILEVS, V. CALO, J. COTTRELL, T. HUGHES, A. REALI, AND G. SCOVAZZI, *Variational multiscale residual-based turbulence modeling for large eddy simulation of incompressible flows*, Comput. Methods Appl. Mech. Engrg., 197 (2007), pp. 173–201.
[3] O. BOTELLA, R. PEYRET, AND Y. DAOQI, *Benchmark spectral results on the lid-driven cavity flow*, Comput. & Fluids, 27 (1998), pp. 421–433.
[4] M. BRAACK AND E. BURMAN, *Local projection stabilization for the Oseen problem and its interpretation as a variational multiscale method*, SIAM J. Numer. Anal., 43 (2006), pp. 2544–2566.
[5] M. BRAACK, E. BURMAN, V. JOHN, AND G. LUBE, *Stabilized finite element methods for the generalized Oseen problem*, Comput. Methods Appl. Mech. Engrg., 196 (2007), pp. 853–866.
[6] M. BRAACK AND T. RICHTER, *Solutions of 3D Navier-Stokes benchmark problems with adaptive finite elemens*, Comput. & Fluids, 35 (2006), pp. 372–392.

ETNA
Kent State University
etna@mcs.kent.edu

[7] A. BROOKS AND T. HUGHES, *Streamline upwind/Petrov-Galerkin formulations for convection dominated flows with particular emphasis on the incompressible Navier-Stokes equations*, Comput. Methods Appl. Mech. Engrg., 32 (1982), pp. 199–259.
[8] E. BURMANN AND P. HANSBO, *Edge stabilization for Galerkin approximations of convection-diffusion problems*, Comput. Methods Appl. Mech. Engrg., 193 (2004), pp. 1437–1453.
[9] R. CODINA, *Analysis of a stabilized finite element approximation of the Oseen equations using orthogonal subscales*, Appl. Numer. Math., 58 (2008), pp. 264–283.
[10] C. DOHRMANN AND P. BOCHEV, *A stabilized finite element method for the Stokes problem based on polynomial pressure projections*, Internat. J. Numer. Methods Fluids, 46 (2004), pp. 183–201.
[11] E. ERTURK, T. C. CORKE, AND C. GOKCOL, *Numerical solutions of 2-D steady incompressible driven cavity flow at high Reynolds numbers*, Internat. J. Numer. Methods Fluids, 48 (2005), pp. 747–774.
[12] U. GHIA, K. GHIA, AND C. SHIN, *High-Re solutions for incompressible flow using the Navier-Stokes equtions and a multigrid method*, J. Comput. Phys., 48 (1982), pp. 387–411.
[13] V. GRAVEMEIER, *The variational multiscale method for laminar and turbulent flow*, Arch. Comput. Methods Engrg., 13 (2006), pp. 249–324.
[14] J.-L. GUERMOND, *Stabilization of Galerkin approximations of transport equations by subgrid modelling*, M2AN Math. Model. Numer. Anal., 33 (1999), pp. 1293–1316.
[15] T. HUGHES, L. MAZZEI, AND K. JANSSEN, *Large eddy simulation and the variational multiscale method*, Comput. Vis. Sci., 3 (2000), pp. 47–59.
[16] V. JOHN AND S. KAYA, *A finite element variational multiscale method for the Navier-Stokes equations*, SIAM J. Sci. Comput., 26 (2005), pp. 1485–1503.
[17] V. JOHN, G. MATTHIES, AND J. RANG, *A comparison of time-discretization/linearization approaches for the incompressible Navier-Stokes equations*, Comput. Meths. Appl. Mech. Engrg., 195 (2006), pp. 5995–6010.
[18] C. JOHNSON AND J. SARANEN, *Streamline diffusion methods for the incompressible Euler and Navier-Stokes equations*, Math. Comp., 47 (1986), pp. 1–18.
[19] J. LÖWE, *Local projection stabilization for incompressible flow problems* (in German), Master Thesis, Department of Mathematics, Georg-August University Göttingen, 2008.
[20] G. LUBE AND G. RAPIN, *Residual-based stabilized higher-order FEM for a generalized Oseen problem*, Math. Models Methods Appl. Sci., 16 (2006), pp. 949–966.
[21] G. MATTHIES, P. SKRZYPACZ, AND L. TOBISKA, *A unified convergence analysis for local projection stabilizations applied to the Oseen problem*, M2AN Math. Model. Numer. Anal., 41 (2007), pp. 713–742.
[22] R. PAWLOWSKI, J. SHADID, J. SIMONIS, AND H. WALKER, *Globalization techniques for Newton-Krylov methods and applications to the fully coupled solution of the Navier-Stokes equations*, SIAM Rev., 48 (2006), pp. 700–721.
[23] G. RAPIN AND J. LÖWE, *Local projection stabilizations for inf-sup stable finite elements applied to the Oseen problem*, submitted, 2007.
[24] H.-G. ROOS, M. STYNES, AND L. TOBISKA, *Numerical Methods for Singularly Perturbed Differential Equations*, Springer, Berlin, 1996.
[25] S. SCHMALJOHANN, *Local projection stabilization for the Oseen problem* (in German), Master Thesis, Department of Mathematics, Ruhr-Universität Bochum, 2007.
[26] L. SCOTT AND S. ZHANG, *Finite element interpolation of nonsmooth functions satisfying boundary conditions*, Math. Comp., 54 (1990), pp. 483–493.
[27] L. ZHANG, *A second-order upwinding finite difference scheme for the steady Navier-Stokes equations in primitive variables in a driven cavity with a multigrid solver*, M2AN Math. Model. Numer. Anal., 24 (1990), pp. 133–150.